This is the author's peer reviewed, accepted manuscript. However, the online version of record will be different from this version once it has been copyedited and typeset. PLEASE CITE THIS ARTICLE AS DOI: 10.1063/5.0173047

Assessment of the Partial Saddle Point Approximation in Field-Theoretic Polymer Simulations

Timothy Quah, ¹ Kris T. Delaney, ² and Glenn H. Fredrickson ^{1, 2, 3}

¹⁾Department of Chemical Engineering, University of California, Santa Barbara, California 93106, USA

²⁾Materials Research Laboratory, University of California, Santa Barbara, California 93106, USA

³⁾Materials Department, University of California, Santa Barbara, California 93106, USA

(*Electronic mail: ghf@ucsb.edu)

(Dated: 5 October 2023)

Assessment of the Partial Saddle Point Approximation in Field-Theoretic Polymer Simulations

Field-theoretic simulations are numerical treatments of polymer field theory models that go beyond the mean-field (SCFT) level and have successfully captured a range of mesoscopic phenomena. Inherent in molecularly-based field theories is a "sign problem" associated with complex-valued Hamiltonian functionals. One route to field-theoretic simulations utilizes the complex Langevin (CL) method to importance sample complex-valued field configurations to bypass the sign problem. Although CL is exact in principle, it can be difficult to stabilize in strongly fluctuating systems. An alternate approach for blends or block copolymers with two segment species is to make a "partial saddle point approximation" (PSPA) in which the stiff pressure-like field is constrained to its mean-field value, eliminating the sign problem in the remaining field theory, allowing for traditional (real) sampling methods. The consequences of the partial saddle point approximation are relatively unknown, and direct comparisons between the two methods are limited. Here, we quantitatively compare thermodynamic observables, order-disorder transitions, and periodic domain sizes predicted by the two approaches for a weakly compressible model of AB diblock copolymers. Using Gaussian fluctuation analysis, we validate our simulation observations, finding that the partial saddle point approximation incorrectly captures trends in fluctuation corrections to certain thermodynamic observables, microdomain spacing, and location of order-disorder transitions. For incompressible models with contact interactions, we find similar discrepancies between the predictions of CL and PSPA, but these can be minimized by regularization procedures such as Morse calibration. These findings mandate caution in applying the PSPA to broader classes of soft-matter models and systems.

This is the author's peer reviewed, accepted manuscript. However, the online version of record will be different from this version once it has been copyedited and typeset.

PLEASE CITE THIS ARTICLE AS DOI: 10.1063/5.0173047

PLEASE CITE THIS ARTICLE AS DOI: 10.1063/5.0173047

Assessment of the Partial Saddle Point Approximation in Field-Theoretic Polymer Simulations

INTRODUCTION I.

Polymer field theories have provided considerable insight into the equilibrium self-assembly behavior of broad classes of inhomogeneous polymers, notably block copolymers and polymer blends. Most commonly, the field theories are treated with a mean-field approximation, also known as self-consistent field theory (SCFT). 1-5 A more refined approach is a field-theoretic simulation (FTS), which is a numerical treatment of the field theory without any simplifying approximations.⁶⁻⁹ FTS samples field fluctuations that depart from the mean-field (or saddle point) configuration and can capture strongly correlated phenomena such as unbinding transitions, fluctuation-induced changes in the order of phase transitions, and charge-driven polyelectrolyte condensation.

Numerical implementation of FTS is challenged by the fact that molecularly-derived field theories have a complex-valued Hamiltonian functional H, so the Boltzmann-like weight $\exp(-H)$ is not positive definite and suffers a "sign problem." Traditional Monte Carlo methods for sampling such high-dimensional complex distributions are ineffective, so alternative approaches must be devised. Over the past 20 years, two separate paths to conducting field-theoretic polymer simulations have emerged: one based on a method known as complex Langevin sampling (CL) that in principle makes no approximations, ^{4,6,7,10–14}, and a second method that approximates one of the fields using a "partial saddle point approximation" (PSPA), which renders the resulting statistical weight positive definite and enables conventional Monte Carlo or (real) Langevin sampling. 15-21 Both FTS methods have been successfully applied to obtain fluctuation-corrected phase diagrams of block copolymers^{13,22-26} and microemulsion-forming ternary polymer blends²⁷⁻²⁹. In addition, CLbased field-theoretic simulations have enabled studies of "bricks and mortar" emulsion phases^{30,31} in mikto-arm block copolymer alloys, the structure and assembly of salt-doped diblock melts³², nematic ordering in bottlebrush polymers³³, and complexation of oppositely charged polyelectrolyte and polyampholyte solutions^{34–38}.

CL-based field-theoretic simulations have the advantage of being approximation free, but complex Langevin trajectories can be difficult to stabilize in certain classes of problems. In contrast, the PSPA approach provides for stable sampling, but it is limited to blends or solutions with only two monomer or solvent species and the impact of the partial saddle point approximation on structural and thermodynamic predictions is largely unknown. Here we provide a detailed, quantitative comparison of the two methods for the specific case of a diblock copolymer melt model that is

PLEASE CITE THIS ARTICLE AS DOI: 10.1063/5.0173047

Assessment of the Partial Saddle Point Approximation in Field-Theoretic Polymer Simulations amenable to study by both techniques.

The theoretical basis for the particular AB diblock copolymer models employed is detailed in the next section, but it helpful to first clarify the nature of the approximation involved in the PSPA and the approach to sampling field fluctuations in both methods. The canonical partition function of standard models of diblock copolymer melts can be expressed in terms of two auxiliary fields $w_{\pm}({\bf r}) \text{ as}^{4,39}$

$$Z_{\rm C}(T,V,n) = \mathscr{Z}_0 \int Dw_+ \int Dw_- e^{-H[w_+,w_-]}$$
(1)

Here, \mathscr{Z}_0 is a term that includes the ideal-gas contribution and Gaussian integral normalizing denominator terms, w_+ is a pressure-like field that resists total density variations in the melt, and w_{-} is an exchange field that determines instantaneous composition profiles (i.e., the relative spatial distribution of A and B block segments). The two integrals in Eq. (1) are functional integrals taken along the real axis for both fields and the Hamiltonian functional $H[w_+, w_-]$ is complex-valued along this integration path. The specific form of H is deferred to the next section.

The simplest method of analyzing Eq. (1) invokes a mean-field (or SCFT) approximation, which assumes that a single field configuration (w_{+}^{*}) and w_{-}^{*} dominates the partition function. Such a mean-field configuration represents a saddle point in the complex plane of the Hamiltonian functional and satisfies the stationary conditions:

$$\left. \frac{\delta H[w_+, w_-]}{\delta w_-(\mathbf{r})} \right|_{w^*} = 0 \tag{2}$$

$$\left. \frac{\delta H[w_+, w_-]}{\delta w_+(\mathbf{r})} \right|_{w_{\pm}^*} = 0 \tag{3}$$

The saddle point value of the pressure field w_{+}^{*} proves to be pure imaginary, while w_{-}^{*} is purely real and all physical observables are likewise real. This includes the mean-field approximation to the Helmholtz free energy, $\beta A = H[w_+^*, w_-^*]$.

The mean-field approximation (SCFT) evidently neglects field fluctuations away from the saddle point, whose strength is controlled by a dimensionless chain concentration $C = nR_g^3/V$ (n is the number of polymers, R_g is the unperturbed radius of gyration of a copolymer, and V is the system volume) that multiplies every term in the Hamiltonian and serves as a Ginzburg parameter. SCFT is thus most accurate in the limit where $C \gg 1$, i.e. the case of dense melts of long polymer chains. We do not correct for fluctuation-induced changes to C through renormalization of the statistical segment length b. ⁴⁰ In our work, the dimensionless chain concentration C is related to a

PLEASE CITE THIS ARTICLE AS DOI: 10.1063/5.0173047

Assessment of the Partial Saddle Point Approximation in Field-Theoretic Polymer Simulations

"bare" invariant degree of polymerization⁴¹ $\bar{N}=6^3C^2=\rho_0^2b^6N$ that is expressed entirely in bare model parameters. Most studies applying the PSPA use a renormalized b parameter and hence \bar{N} obtained from a Morse calibration procedure. Experimentally relevant dimensionless chain concentrations for a block copolymer range from $C\approx 1-5$. As previously mentioned, a major challenge in sampling such molecularly-derived field theories is the sign problem that arises from a complex-valued Hamiltonian, leading to Boltzmann weights that are not positive-definite. The partial saddle point approximation (PSPA)¹⁶ bypasses this problem by approximating the w_- dependent w_+ integral with a saddle point approximation while retaining the functional integral over w_- , i.e.

$$Z_C(T,V,n) = \mathscr{Z}_0 \int Dw_- \int Dw_+ e^{-H[w_+,w_-]}$$

$$\approx \mathscr{Z}_0 \int Dw_- e^{-H_p[w_-]}$$
(4)

$$H_p[w_-] \equiv H[w_+^*[w_-], w_-] \tag{5}$$

Here $w_+^*[w_-]$ denotes the saddle point value of the w_+ field at fixed w_- , which is obtained by numerically solving the equation

$$\left. \frac{\delta H[w_+, w_-]}{\delta w_+(\mathbf{r})} \right|_{w_+^*} = 0 \tag{6}$$

with w_- specified. Crucially, the PSPA renders $w_+^*[w_-]$ pure imaginary and the effective Hamiltonian $H_p[w_-]$ purely real, so the sign problem is avoided in the second line of Eq. (4). The resulting approximate theory in the single real field w_- can thus be numerically simulated using any stochastic method capable of efficient sampling of high-dimensional, real-valued probability distributions, e.g. Monte Carlo or (real) Langevin dynamics.

Real Langevin dynamics is the most commonly used method for sampling field configurations w_- within the PSPA. This is a fictitious dynamics used to generate a Markov chain of field configurations representative of the Boltzmann distribution $\exp(-H_p[w_-])$. At steady state, fictitious-time-averages over the Markov chain can be used to approximate ensemble averages of the PSPA field theory defined by Eq. (4). In such a sampling scheme, Langevin updates of the w_- field are staggered with numerical solutions of Eq. (6) to obtain the partial saddle point field $w_+^*[w_-]$ necessary to evaluate $H_p[w_-]$. Specifically, the coupled scheme involves the solution of the following

Chemical Physics ACC

This is the author's peer reviewed, accepted manuscript. However, the online version of record will be different from this version once it has been copyedited and typeset

PLEASE CITE THIS ARTICLE AS DOI: 10.1063/5.0173047

Assessment of the Partial Saddle Point Approximation in Field-Theoretic Polymer Simulations

equations

$$\left. \frac{\delta H[w_+, w_-]}{\delta w_+(\mathbf{r}, t)} \right|_{w_+^*} = 0 \tag{7}$$

$$\frac{\partial w_{-}(\mathbf{r},t)}{\partial t} = -\frac{\delta H_p[w_{-}]}{\delta w_{-}(\mathbf{r},t)} + \eta(\mathbf{r},t)$$
(8)

where t is the fictious time variable and $\eta(\mathbf{r},t)$ is a real Gaussian white noise. The statistical properties of the noise are defined by its first two moments

$$\langle \boldsymbol{\eta} \left(\mathbf{r}, t \right) \rangle = 0 \tag{9}$$

$$\langle \eta(\mathbf{r},t) \eta(\mathbf{r}',t') \rangle = 2\delta(t-t')\delta(\mathbf{r}-\mathbf{r}')$$
 (10)

where the covariance in Eq. (10) is chosen in accordance with the fluctuation-dissipation theorem.

The alternative to the partial saddle point approach is to retain the *exact* field theory of Eq. (1) and tackle the sign problem using complex Langevin (CL) dynamics. In contrast to real Langevin, CL is a fictitious stochastic dynamics that explores complex-valued field configurations and in this instance generates a Markov chain of states representative of the complex distribution $\exp(-H[w_+, w_-])$. The CL equations are not guaranteed to converge to a steady state, but if convergent, it can be proven that fictitious-time averages using the Markov chain are equivalent to ensemble averages of the full field theory given in Eq. (1).^{46,47} The complex Langevin dynamical equations are as follows:^{7,39}

$$\frac{\partial w_{-}(\mathbf{r},t)}{\partial t} = -\frac{\delta H[w_{+},w_{-}]}{\delta w_{-}(\mathbf{r},t)} + \eta_{-}(\mathbf{r},t)$$
(11)

$$\frac{\partial w_{+}(\mathbf{r},t)}{\partial t} = -\frac{\delta H[w_{+},w_{-}]}{\delta w_{+}(\mathbf{r},t)} + \eta_{+}(\mathbf{r},t)$$
(12)

where $\eta_{\pm}(\mathbf{r},t)$ are independent real Gaussian white noises with statistical properties defined by the moments given in Eqs. (9) and (10). Within the complex Langevin scheme, both w_{+} and w_{-} are updated simultaneously. With the noise terms omitted, Eqs. (11) and (12) reduce to a deterministic descent scheme for finding saddle point solutions, i.e. solutions of Eqns. (2) and (3). More generally, the stochastic CL equations serve to importance sample the full complex distribution of field states. At large chain concentration, $C \gg 1$, CL trajectories are usually concentrated on constant phase paths in the close vicinity of saddle points, but in cases of stronger fluctuations ($C \lesssim 1$) CL trajectories can sample states far removed from saddle points. Under such conditions of strong fluctuations, the CL equations can prove difficult to stably integrate.⁴⁸

PLEASE CITE THIS ARTICLE AS DOI: 10.1063/5.0173047

Assessment

Assessment of the Partial Saddle Point Approximation in Field-Theoretic Polymer Simulations

Both methods of conducting FTS simulations have qualitatively captured the experimental observation that fluctuation contributions lead to shifts in the order-disorder transition in linear diblock copolymers that increase with decreasing C. However, there have been only two *quantitative* comparisons between fully fluctuating and partial saddle-point approximation field-theoretic simulations; one was conducted in a ternary blend of a AB diblock copolymer with A and B homopolymer and the other in thin films of molten AB diblock copolymer. Both works showed good agreement between the CL and PSPA methods in a region where fluctuation corrections are small ($C \gg 1$). The diblock study showed that even in the weakly fluctuating regime, there were perceptible differences between CL and PSPA. To date, the partial saddle point approximation has not been tested in the important regime of $C \lesssim 10$ and we lack a theoretical argument to clearly establish the conditions that would justify its use. In the absence of such theoretical guidance, here we embark on a direct numerical comparison of the two methods to better understand the consequences of invoking the partial saddle point approximation.

II. THEORETICAL AND NUMERICAL METHODS

In this section we detail the specific models of AB diblock copolymer melts that will used as a test bed for the PSPA-CL comparison and summarize the theoretical and numerical methods employed. Two diblock copolymer models are considered: *Model I*, an incompressible melt with continuous Gaussian chains and contact non-bonded interactions and, *Model II*, a weakly compressible melt with continuous Gaussian chains and repulsive Gaussian non-bonded interactions. Model I is a standard model used in polymer physics,³ but is ultraviolet divergent, so requires care to extract thermodynamic properties independent of fine scale artifacts of the computational grid. Model II is ultraviolet convergent^{11,13} and can be used directly to obtain grid-independent properties.

Our investigation of the validity of the partial saddle point approximation focuses primarily on the weakly compressible model because it is mathematically well-defined and free of UV divergences. A more limited study of the incompressible model is contained in the supplementary information.

PLEASE CITE THIS ARTICLE AS DOI: 10.1063/5.0173047

Assessment of the Partial Saddle Point Approximation in Field-Theoretic Polymer Simulations

Model I: Unregularized Incompressible Model

We first consider the model of incompressible AB-diblock copolymers with contact segmental interactions.^{3,4} Its canonical partition function $Z_{\mathbb{C}}(n,V,T)$ is given by

$$Z_{C}(n, V, T) = \frac{1}{\lambda_{T}^{3nN} n!} \prod_{i=1}^{n} \int D\mathbf{r}_{i} e^{-\beta U_{0} - \beta U_{1}} \prod_{\mathbf{r}} \delta(\hat{\rho}_{A}(\mathbf{r}) + \hat{\rho}_{B}(\mathbf{r}) - \rho_{0})$$
(13)

$$\beta U_0 = \frac{3}{2b^2} \sum_{j=1}^n \int_0^N ds \left| \frac{d\mathbf{r}_j(s)}{ds} \right|^2 \tag{14}$$

$$\beta U_1 = \frac{\chi}{\rho_0} \int d\mathbf{r} \, \hat{\rho}_{A}(\mathbf{r}) \hat{\rho}_{B}(\mathbf{r})$$
(15)

where $\beta \equiv 1/(k_B T)$ is the inverse of the thermal energy, T is the temperature, and λ_T is the thermal de Broglie wavelength of a polymer segment. The potential energy in Eq. (13) is composed of an elastic bonded term (βU_0) and a contact non-bonded interaction term (βU_1). We have used the continuous Gaussian chain model for βU_0 (shown in Eq. (14)) with N the total number of segments on each diblock copolymer and b the statistical segment length. The strength of the interaction term βU_1 , (shown in Eq. (15)) is dictated by a Flory Huggins χ parameter between A and B segments. The final factor in the integrand of Eq. 13 is an incompressibility constraint that fixes the sum of the microscopic densities of A and B segments locally at each point r to the average total segment density $\rho_0 = Nn/V$. The microscopic densities for the two segment species are defined as

$$\hat{\rho}_{A}(\mathbf{r}) = \sum_{i=1}^{n} \int_{0}^{fN} ds \, \delta(\mathbf{r} - \mathbf{r}_{i}(s))$$
 (16)

$$\hat{\rho}_{\mathrm{B}}(\mathbf{r}) = \sum_{i=1}^{n} \int_{fN}^{N} ds \, \delta(\mathbf{r} - \mathbf{r}_{i}(s))$$
 (17)

with f the volume fraction of type A segments on each diblock chain. By introducing $\hat{\rho}_{+}(\mathbf{r}) =$ $\hat{\rho}_A(\mathbf{r}) \pm \hat{\rho}_B(\mathbf{r})$ and using two auxiliary fields $w_{\pm}(\mathbf{r})$ (conjugate to $\hat{\rho}_{\pm}$) to decouple the U_1 interaction and exponentiate the incompressibility constraint, we obtain the following field theory:

$$Z_{C}(n,V,T) = \mathcal{Z}_{0} \int Dw_{+} \int Dw_{-} e^{-H[w_{+},w_{-}]}$$

$$H[w_{+},w_{-}] =$$

$$-C \int d\mathbf{r} iw_{+}(\mathbf{r}) + \frac{C}{\chi_{AB}N} \int d\mathbf{r} w_{-}^{2}(\mathbf{r})$$

$$-C\hat{V} \ln Q[w_{A},w_{B}]$$

$$(18)$$

This is the author's peer reviewed, accepted manuscript. However, the online version of record will be different from this version once it has been copyedited and typeset.

PLEASE CITE THIS ARTICLE AS DOI: 10.1063/5.0173047

Assessment of the Partial Saddle Point Approximation in Field-Theoretic Polymer Simulations

Here, \mathcal{Z}_0 is a term that includes the ideal gas partition function of n noninteracting polymers, and a Gaussian functional integral denominator.^{7,13} All lengths have been scaled by the unperturbed radius of gyration $R_g = b(N/6)^{1/2}$, $C = nR_g^3/V$ is the dimensionless chain concentration introduced above, and $\hat{V} = V/R_g^3$ is the dimensionless volume. Since C multiplies all three terms in the effective Hamiltonian of Eq (19), it is clear that it plays the role of a Ginzburg parameter regulating the strength of fluctuations about saddle point (mean field) solutions.

The functional $Q[w_A, w_B]$ is a normalized partition function of a single copolymer experiencing the species fields w_A and w_B , which are linear combinations of the auxiliary fields w_{\pm} ,

$$w_A \equiv iw_+ - w_-, \ w_B \equiv iw_+ + w_-$$
 (20)

Q can be evaluated from the formula⁴ $Q = (1/\hat{V}) \int d\mathbf{r} q(\mathbf{r}, 1)$, where $q(\mathbf{r}, s)$ is a single-chain propagator for a chain experiencing the w_A/w_B fields. The propagator $q(\mathbf{r},s;[w_A,w_B])$ satisfies the modified diffusion equation

$$\frac{\partial}{\partial s}q(\mathbf{r},s) = (\nabla^2 - w(\mathbf{r},s))q(\mathbf{r},s)$$
 (21)

$$\frac{\partial}{\partial s} q(\mathbf{r}, s) = (\nabla^2 - w(\mathbf{r}, s)) q(\mathbf{r}, s)$$

$$w(\mathbf{r}; s) = \begin{cases} w_A(\mathbf{r}) & 0 \le s \le f \\ w_B(\mathbf{r}) & f < s \le 1 \end{cases}$$
(21)

with initial condition $q(\mathbf{r},0)=1$. We note that the chain contour variable s has been scaled by N and lengths by R_g in these expressions.

As mentioned previously, this incompressible model with contact repulsions is UV divergent and does not possess a well-defined continuum limit. This is manifested by some thermodynamic properties (such as the chemical potential) being infinite. UV divergences for an observable occur when the high-wavenumber modes of field fluctuations are not sufficiently damped and often arise from an inadequate description of short-ranged physics. Two strategies have been used to "regularize," i.e. mitigate, UV divergences in the model: impose a high-wavenumber cutoff or modify the short scale physics of the model such that high-wavenumber fluctuation modes are suppressed. The latter strategy is deferred to the next section, while the former is implemented by discretizing the theory onto a spatial grid. Such a regularization method yields finite observables, but their values are sensitive to the spatial resolution of the lattice. ^{23,26,49} This can create challenges in locating order-disorder (and especially order-order) phase boundaries, where different lattice discretizations would normally be used for the phases being analyzed. Nonetheless, a

PLEASE CITE THIS ARTICLE AS DOI: 10.1063/5.0173047

Assessment of the Partial Saddle Point Approximation in Field-Theoretic Polymer Simulations

variety of methods have been developed for managing UV divergences in the present model 19,23,26 and isolating universal order-disorder phase behavior. 50,51

Model II: Regularized Weakly Compressible Model

The alternative to imposing a lattice cutoff is to modify the model such that UV divergences are eliminated. The primary sources of UV divergences in the model described in Eq. (19) arise from continuous Gaussian chain statistics, the point-like contact interactions, and the constraint of local incompressibility. The continuous Gaussian chain statistics can be easily remediated by referencing all thermodynamic observable to an ideal gas reference of continuous Gaussian chains. Similarly, replacing contact repulsions among non-bonded pairs of segments with a repulsive Gaussian pair potential can serve to eliminate UV divergences. As discussed elsewhere, 7,11,52 this is equivalent to smearing (convolving) the microscopic segment densities by a Gaussian with half the variance of the pair potential. In the model described here, we smear with the normalized Gaussian, $\Gamma(r) = (2\pi a^2)^{-3/2} \exp(-r^2/2a^2)$, where r is the radial coordinate from the segment center, and a is the width of the spread, proportional to the interaction range. Finally, instead of strictly enforcing local incompressibility, we harmonically penalize deviations from the target density.⁵³ The resulting model in the particle representation has the following form:

$$Z_{\rm C}(n, V, T) = \frac{1}{\lambda_{\rm T}^{3nN} n!} \prod_{i=1}^{n} \int D\mathbf{r}_{i} e^{-\beta U_{0} - \beta U_{1} - \beta U_{2}}$$
(23)

$$\beta U_1 = \frac{\chi}{\rho_0} \int d\mathbf{r} \, \check{\rho}_{A}(\mathbf{r}) \check{\rho}_{B}(\mathbf{r})$$
 (24)

$$\beta U_2 = \frac{\zeta}{2\rho_0} \int d\mathbf{r} \left(\check{\rho}_{A}(\mathbf{r}) + \check{\rho}_{B}(\mathbf{r}) - \rho_0 \right)^2$$
 (25)

The potential energy in Eq. (23) is composed of the bonded elasticity (βU_0) and non-bonded interactions (βU_1 and βU_2). The term βU_0 (Eq. (14)) remains the same as in the incompressible model. The first interaction term βU_1 (Eq. (24)) is again parameterized by a Flory Huggins χ parameter between A and B segments. In contrast to Eq. (15), the current model adopts smeared segments whose densities are related to the microscopic densities (Eqs. (16 - 17)) by the three-dimensional convolution operation $\check{\rho}_j(\mathbf{r}) = \Gamma \star \hat{\rho}_j \equiv \int d\mathbf{r}' \; \Gamma(|\mathbf{r} - \mathbf{r}'|) \hat{\rho}_j(\mathbf{r}')$. The second interaction term βU_2 (Eq. (25)) harmonically penalizes local deviations of the total density from the target density ρ_0 with a stiffness parameterized by the Helfand compressibility coefficient ζ . ^{12,13,54} By following similar steps described for the incompressible model and employing the same dimensionless scal-

PLEASE CITE THIS ARTICLE AS DOI: 10.1063/5.0173047

ings, we obtain a field-theoretic represesentation of the weakly-incompressible model:

$$Z_{C}(n,V,T) = \mathscr{Z}_{0} \int Dw_{+} \int Dw_{-}e^{-H[w_{+},w_{-}]}$$

$$H[w_{+},w_{-}] =$$

$$\frac{C}{\chi_{AB}N + 2\zeta N} \int d\mathbf{r} \left(w_{+}^{2}(\mathbf{r}) - 2i\zeta Nw_{+}(\mathbf{r})\right)$$

$$+ \frac{C}{\chi_{AB}N} \int d\mathbf{r} w_{-}^{2}(\mathbf{r}) - C\hat{V} \ln Q[\Gamma \star w_{A}, \Gamma \star w_{B}]$$

$$(26)$$

Evidently the unregularized incompressible model, Eq. (19), is recovered in the limit where $\zeta N \rightarrow$ ∞ and $a \rightarrow 0$.

Gaussian Fluctuation Analysis

We utilize analytical Gaussian fluctuation analysis in the weakly-inhomogenous regime to validate and confirm our simulation observations. This approach deforms the contour of the functional integrals to a (locally) constant phase contour through the homogeneous saddle point and expands the Hamiltonian functional to quadratic order in the deviations of the w_{\pm} fields away from that point. The simplified field theory has Gaussian functional integrals that can be analytically performed, yielding approximate expressions for the partition function and free energy. These formulas are valid only in the homogeneous disordered phase of a block copolymer melt, where field fluctuations are concentrated in the basin of the homogeneous saddle point, and are most accurate at large C, when the fluctuations are weak in amplitude. In the case of Model II described by Eqs. (26) and (27), we recover a previously reported Gaussian fluctuation formula. 13 Since the underlying model is UV convergent, we report the continuum thermodynamic limit that uses an integral rather than a sum over reciprocal lattice vectors k. Detailed derivations are included in the supplementary information. The fluctuation-corrected Helmholtz free energy per chain is given by

$$\frac{\beta F_{\text{full}}}{n} = \frac{\beta F_{\text{IG}}}{n} + \chi N f(1 - f)
+ \frac{1}{4\pi^2 C} \int_0^\infty dk \, k^2 \ln\left[1 + (2\chi N \hat{g}_{\text{AB}}(k^2) + \zeta N \hat{g}_{\text{D}}(k^2))\hat{\Gamma}^2(k^2) \right]
+ \chi N(\chi N + 2\zeta N)(\hat{g}_{\text{AB}}^2(k^2) - \hat{g}_{\text{AA}}(k^2)\hat{g}_{\text{BB}}(k^2))\hat{\Gamma}^4(k^2) \right]$$
(28)

where $\hat{\Gamma}(k^2) = \exp[-k^2(a/R_g)^2/2]$ is the three dimensional Fourier transform of $\Gamma(r)$. The first term is the intensive free energy of an ideal gas of continuous Gaussian chains; the second is

PLEASE CITE THIS ARTICLE AS DOI: 10.1063/5.0173047

Assessment of the Partial Saddle Point Approximation in Field-Theoretic Polymer Simulations

the mean-field contribution. The final term is a Gaussian fluctuation correction where $\hat{g}_{AA}(k^2)$, $\hat{g}_{BB}(k^2)$, $\hat{g}_{AB}(k^2)$, and $\hat{g}_{D}(k^2)$ are Debye functions that arise from the expansion of the singlechain partition function. These are given by

$$\hat{g}_{AA}(k^2) = \frac{2}{k^4} \left[\exp(-fk^2) + fk^2 - 1 \right]$$
 (29)

$$\hat{g}_{BB}(k^2) = \frac{2}{k^4} \left[\exp(-(1-f)k^2) + (1-f)k^2 - 1 \right]$$
(30)

$$\hat{g}_{AB}(k^2) = \frac{1}{k^4} \left[\exp(-fk^2) - 1 \right] \left[\exp(-(1-f)k^2) - 1 \right]$$
 (31)

$$\hat{g}_{D}(k^{2}) = \frac{2}{k^{4}} \left[\exp(-k^{2}) + k^{2} - 1 \right]$$
(32)

From Eq. (28), we can use standard thermodynamic relationships to obtain additional quantities such as chemical potential μ and osmotic pressure P. The fluctuation contribution in Eq. (28) given by the reciprocal-space integral is divergent in the limit of $a \to 0$ and $\zeta N \to \infty$, confirming that incompressibility and point-like interactions are indeed the problematic sources of UV divergence within the conventional (incompressible and unsmeared) Model I.

We repeat the Gaussian fluctuation analysis for the partial saddle point approximation by expanding the saddle point approximation for w_+ to second order in powers of w_- to obtain an effective Hamiltonian solely dependent on w_{-} . This leads to the free energy expression

$$\frac{\beta F_{\text{partial}}}{n} = \frac{\beta F_{\text{IG}}}{n} + \chi N f(1 - f)
+ \frac{1}{4\pi^2 C} \int_0^\infty dk \, k^2 \ln \left[d(k^2) \left(1 - \frac{\chi N}{2} \left(a(k^2) - b(k^2) e(k^2) + c(k^2) e^2(k^2) \right) \right) \right] (33)$$

where

$$e(k^{2}) = \frac{(\hat{g}_{AA}(k^{2}) - \hat{g}_{BB}(k^{2}))(\chi N + 2\zeta N)\hat{\Gamma}^{2}(k^{2})}{2 + (\chi N + 2\zeta N)\hat{g}_{D}(k^{2})\hat{\Gamma}^{2}(k^{2})}$$

$$d(k^{2}) = \frac{2\zeta N + \chi N}{2\zeta N + \chi N(1 - \bar{\Omega}_{+}^{*2}(k^{2}))}$$
(35)

$$d(k^2) = \frac{2\zeta N + \chi N}{2\zeta N + \chi N (1 - \bar{\Omega}^{*2}(k^2))}$$
(35)

$$a(k^2) = (\hat{g}_{AA}(k^2) + \hat{g}_{BB}(k^2) - 2\hat{g}_{AB}(k^2))\hat{\Gamma}^2(k^2)$$
(36)

$$b(k^2) = 2(\hat{g}_{AA}(k^2) - \hat{g}_{BB}(k^2))\hat{\Gamma}^2(k^2)$$
(37)

$$c(k^2) = \frac{2}{2\zeta N + \gamma N} + \hat{g}_D(k^2)\hat{\Gamma}^2(k^2)$$
(38)

This expression simplifies considerably for the specific case of a symmetric diblock copolymer

PLEASE CITE THIS ARTICLE AS DOI: 10.1063/5.0173047

Assessment of the Partial Saddle Point Approximation in Field-Theoretic Polymer Simulations

melt (f = 1/2) where $e(k^2) = 0$ and $\hat{g}_{AA}(k^2) = \hat{g}_{BB}(k^2)$,

$$\frac{\beta F_{\text{partial}}}{n} = \frac{\beta F_{\text{IG}}}{n} + \frac{\chi N}{4} + \frac{1}{4\pi^2 C} \int_0^\infty dk \, k^2 \ln\left[1 - \chi N\left(\hat{g}_{\text{AA}}(k^2) - \hat{g}_{\text{AB}}(k^2)\right)\hat{\Gamma}^2(k^2)\right] \tag{39}$$

In this particular case, the dependence on ζN is eliminated.

D. Simulation Details

For all calculations involving real and complex Langevin dynamics, we use an exponential time differencing (ETD) scheme^{55,56}. PSPA requires saddle points of the w_+ field for every configuration of w_- ; we utilize the ETD scheme and terminate our search when the L_2 norm of the force is below a tolerance of 10^{-4} .⁵⁷ We use a second-order Strang operator splitting algorithm to solve Eq. 21 with a contour discretization of $\Delta s = 0.01$.^{58,59} To regularize our model, we have picked a moderate Gaussian smearing width $a = 0.2 R_g$, and all our results correspond to the symmetric composition f = 0.5 at various segregation strengths χN and inverse compressibilities ζN .

We evaluate the free energy of the system in both sampling methods using the direct free energy method outlined by Fredrickson and Delaney that computes the Helmholtz free energy using the thermodynamic relationship $F = n \langle \tilde{\mu}[w_{\pm}] \rangle - \langle \tilde{P}[w_{\pm}] \rangle V$, where $\tilde{\mu}[w_{\pm}]$ and $\tilde{P}[w_{\pm}]$ are chemical potential and pressure field operators, respectively. In the case of ordered mesophases, we consider cell size and shape variation at constant concentration c = n/V. Specifically, we seek the equilibrium condition

$$\frac{\partial \beta F(n, \mathbf{h}, T)/V}{\partial \mathbf{h}} \bigg|_{CT} = \frac{\partial \beta F_{\text{ex}}(n, \mathbf{h}, T)/V}{\partial \mathbf{h}} \bigg|_{CT} = 0$$
 (40)

where **h** is the cell tensor that defines the shape and volume $V = \det(\mathbf{h})$ of a parallelpiped cell. The first equality is due to the ideal gas contributions to the free energy density $\beta F/V$ being constant at fixed c; $F_{\rm ex}$ is the Helmholtz free energy in excess of the ideal gas. The second expression in Eq. (40) can be shown to be equal to 14

$$\frac{\partial \beta F_{\text{ex}}(n, \mathbf{h}, T)/V}{\partial \mathbf{h}} \bigg|_{c, T} \mathbf{h}^{T} = c\beta \left\langle \tilde{\mu}_{\text{ex}}(\mathbf{h}; [w_{\pm}]) \right\rangle \mathbf{I} + \beta \left\langle \tilde{\sigma}_{\text{ex}}(\mathbf{h}; [w_{\pm}]) \right\rangle - (\beta A_{\text{ex}}/V) \mathbf{I} \tag{41}$$

ublishing Chemical Physics

This is the author's peer reviewed, accepted manuscript. However, the online version of record will be different from this version once it has been copyedited and typeset

PLEASE CITE THIS ARTICLE AS DOI: 10.1063/5.0173047

Assessment of the Partial Saddle Point Approximation in Field-Theoretic Polymer Simulations

where $\tilde{\mu}_{\rm ex}$ is the excess chemical potential operator, $\tilde{\sigma}_{\rm ex}$ is the excess internal stress operator, and **I** is the unit tensor. For a cell that has been relaxed at fixed volume to a state of isotropic stress $\langle \tilde{\sigma}_{\rm ex}(\mathbf{h}; [w_{\pm}]) \rangle = -P_{\rm ex}\mathbf{I}$ with excess pressure $P_{\rm ex}$, the right side of Eq. (41) vanishes, providing access to both the equilibrium domain size and the Helmholtz free energy.

III. RESULTS

To understand the implications of taking the saddle point approximation from an analytical and simulation perspective, we first study the homogeneous disordered phase of a symmetric diblock melt (f = 0.5) far from the order-disorder transition ($\chi N = 5.0$). We compare the chemical potential μ , osmotic pressure P, and Helmholtz free energy F over four orders of magnitude of the dimensionless chain concentration C. Simulations employed cubic cells of side lengths $L = 3.0R_g$, over a ζN range spanning 50 - 500. Each subplot reports thermodynamic averages computed using complex Langevin (CL) simulations with filled squares and real Langevin simulations invoking the partial saddle point approximation (PSPA) with unfilled triangles. The lines are analytical references from Gaussian fluctuation analysis of the full and approximated (PSPA) models.

Figures 1a, 1b, and 1c demonstrate that the fluctuation contributions (beyond SCFT, including ideal gas terms) to each property differ significantly between methods that use the full field theory and those that invoke the PSPA. Both simulation methods (CL and the PSPA) agree semi-quantitatively with the corresponding analytical Gaussian fluctuation analysis. The predicted full field theory corrections are positive in the chemical potential and Helmholtz free energy and negative of similar magnitude in the osmotic pressure. In contrast, the PSPA corrections are negative in all three thermodynamic quantities. For μ , the fluctuation contribution given by the PSPA is much smaller than predicted by CL. Although the pressure corrections trend correctly, the PSPA severely underestimates the fluctuation corrections by several orders of magnitude. Since we calculate F by combining μ and P, unsurprisingly, the free energy corrections are lower and trend incorrectly. CL predicts that P and μ contribute similarly to F, but the PSPA predicts that μ contributions dominate the free energy. Another trend we observe is in the variations with compressibility: an increase in ζN reduces the compressibility and leads to more significant fluctuation contributions to F. It is also evident that both the analytical and simulation PSPA results are insensitive to compressibility variations, consistent with the lack of ζN dependence in Eq (39).

The incompressible limit of Eqs. (28) and (33) provides additional insights into the PSPA. The

PLEASE CITE THIS ARTICLE AS DOI: 10.1063/5.0173047

Assessment of the Partial Saddle Point Approximation in Field-Theoretic Polymer Simulations

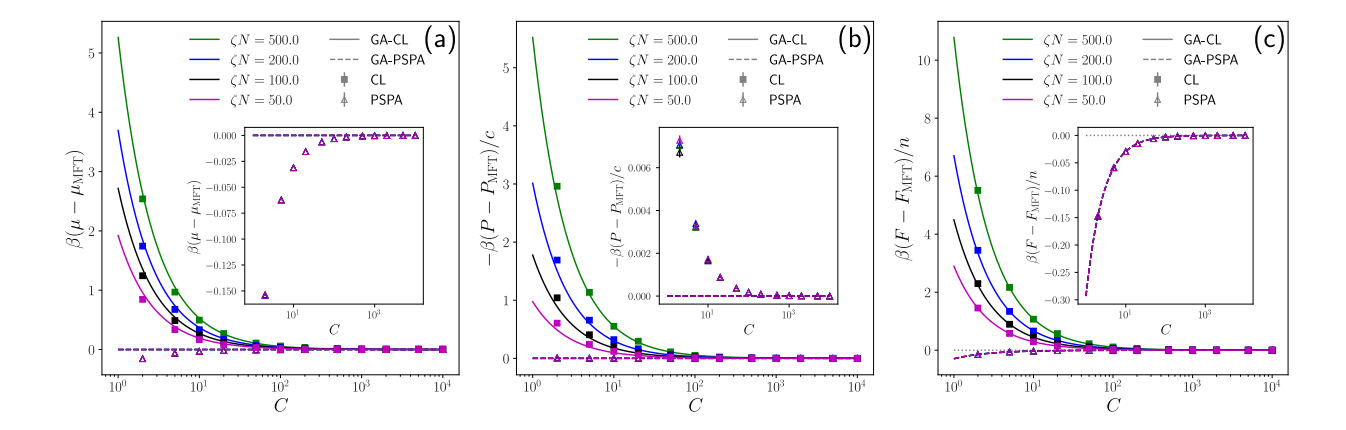


FIG. 1: Comparison of thermodynamic properties in the disordered phase at $\chi N=5.0$ and f=0.5 between fully fluctuating field-theoretic simulations using complex Langevin sampling (CL) and the partial saddle point approximation using real Langevin sampling (PSPA) at different chain concentrations C and inverse compressibilities ζN . The mean-field (MFT or SCFT) contribution to each property, including ideal gas terms, has been subtracted to isolate fluctuation contributions. Lines are from Gaussian fluctuation analysis of the full theory (GA-CL) and with the partial-saddle point approximation (GA-PSPA). The properties studied are (a) chemical potential μ , (b) osmotic pressure P, and (c) intensive Helmholtz free energy F/n. Inset subplots are PSPA results on an expanded scale.

full theory in the Gaussian approximation is divergent for $\zeta N \to \infty$, while the Gaussian approximation for the PSPA is not divergent in the incompressible limit. Nonetheless, the divergence can be eliminated by subtracting the free energy of a system in a reference state, real or hypothetical. A convenient reference state for this purpose is a copolymer melt with $\chi N = 0.0$. Figure 2 shows that when the free energy of the reference state is subtracted, the data of Figure 1c undergoes considerable collapse with the weakly compressible model continuously approaching the behavior of the incompressible model for $\zeta N \to \infty$. The differing behaviors of the full and PSPA treatments of the model are also minimized by this simple regularization. Overall, we see that in the disordered phase, far from the order-disorder transition, the failings of the PSPA can be mitigated by referencing the free energy to a state with $\chi N = 0.0$. We now turn our attention to weakly segregated systems in the vicinity of the order-disorder transition (ODT).

Both FTS methods have been extensively applied to study order-disorder transitions. To understand how they differ, we investigated the melting of a lamellar structure by varying the interaction strength ($\chi \sim T^{-1}$). We set the single chain concentration and compressibility parameters

PLEASE CITE THIS ARTICLE AS DOI: 10.1063/5.0173047

Assessment of the Partial Saddle Point Approximation in Field-Theoretic Polymer Simulations

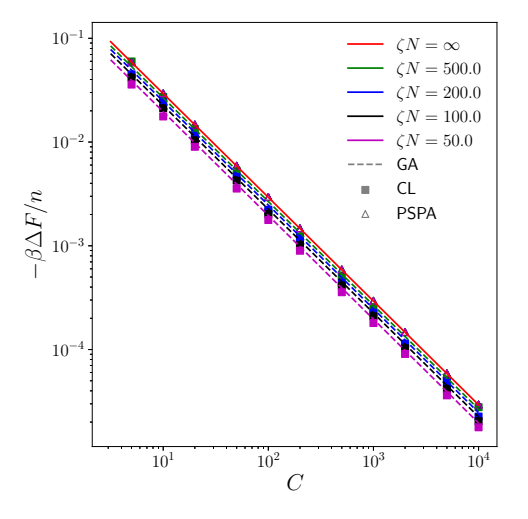


FIG. 2: The free energy data in Figure 1c referenced to a state with $\chi N=0$. The free energy difference shown is defined as $\beta \Delta F/n=\beta (F/n-F_{\chi N=0}/n)-\chi N/4$, a quantity that smoothly approaches the incompressible limit for $\zeta N\to\infty$.

to C = 100 and $\zeta N = 100$ and initialized each stochastic simulation from a three-period lamellar structure obtained by SCFT.

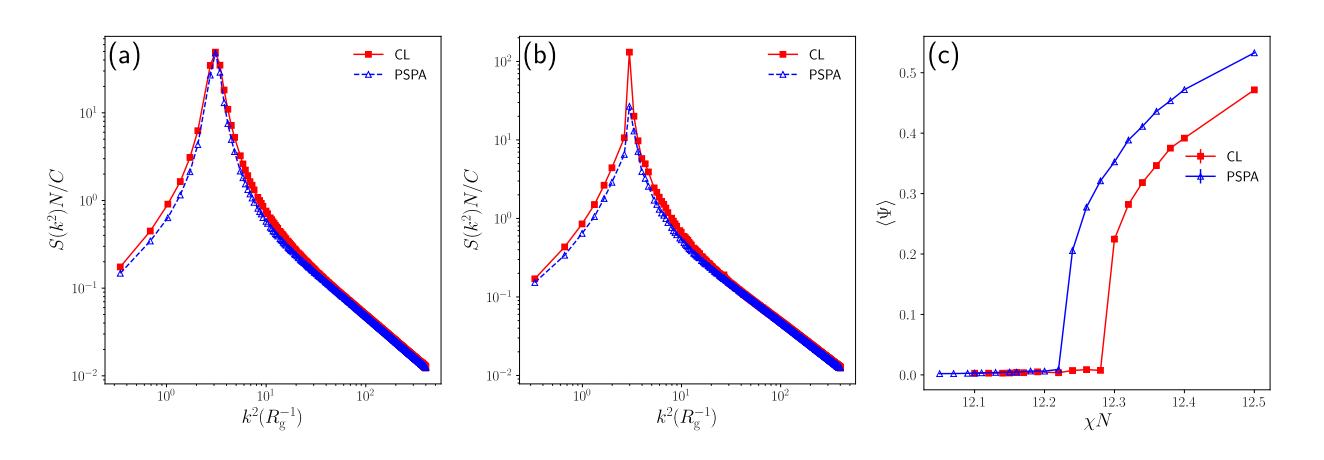


FIG. 3: Comparison of structure factors S(k) at C=100.0 and $\zeta N=100$ between field-theoretic simulations using complex Langevin sampling (CL) and the partial saddle point approximation with real Langevin sampling (PSPA). (a) Disordered phase with $\chi N=12.10$, (b) Ordered lamellar phase (LAM) with $\chi N=12.50$. (c) Melting of the LAM phase by tracking the orientational persistence order parameter Ψ across a range of segregation strengths χN .

In Figure 3a and 3b, we compare the scattering functions S(k) obtained from the CL and PSPA simulation methods at two different interaction strengths: disordered ($\chi N = 12.10$) and ordered

This is the author's peer reviewed, accepted manuscript. However, the online version of record will be different from this version once it has been copyedited and typeset.

PLEASE CITE THIS ARTICLE AS DOI: 10.1063/5.0173047

Assessment of the Partial Saddle Point Approximation in Field-Theoretic Polymer Simulations

 $(\chi N=12.50)$. The CL data are shown with filled red squares, the PSPA data with unfilled blue triangles, and the lines are guides to the eye. Both methods yield similar scattering functions in the disordered regime with peak positions k^* and intensities $S(k^*)$ nearly identical. The data for the weakly-ordered lamellar (LAM) phase shown in Figure (3b) reveals different predictions by the two methods, especially in the peak intensity $S(k^*)$ which is significantly larger in CL compared to PSPA. For both disordered and ordered phases, we observe that CL produces scattering profiles that are broader about the primary peak k^* than those generated by PSPA. The intensity of the peak $(S(k^*))$ is sensitive to the simulation cell size. Both sets of simulations share the same cell dimensions.

In Figure 3c, the melting of the lamellar phase is followed by tracking an orientational persistence order parameter Ψ that is nonzero only in a well-ordered LAM structure. We employ an expression for Ψ that has been previously used to study order-disorder transitions in lamellar diblock copolymers. Two main observations are that the PSPA predicts a lower χN order-disorder transition than CL and, at the same segregation strength, the lamellar structure emerging from PSPA is more ordered than that from CL. This behavior has its origins in the PSPA not sampling the full spectrum of field fluctuations, which leads to smoother field configurations, stronger ordering, and a smaller fluctuation-induced shift of the ODT in comparison with the "exact" CL results.

The location of the ODT can be more precisely determined by comparing the free energies of the LAM and disordered phases, following the "direct" approach recently developed by Fredrickson and Delaney. ¹⁴ Two simulations were run for each interaction strength: one cell initialized from a three-period lamellae seed obtained by SCFT and the other from a homogeneous seed of the same volume. The ODT is determined by interpolating the zero crossing of the free energy difference between the LAM and disordered phases (in Figure 4a at C = 100). We track the order-disorder predictions for the CL and PSPA methods over a series of C ranging from C = 1000 in Figure 4b. Figure 4a shows that the direct free energy method leads to precise ODT predictions that are consistent with the broad transitions identified using the orientational persistence order parameter in Figure (3c). The trend remains that the PSPA underestimates the C0 threshold for the order-disorder transition. In our study of the critical segregation strength over chain concentration C1 spanning 20 – 1000, both methods trend similarly, with C2 predicted by CL and PSPA widens as C3 decreases, with the PSPA consistently underestimating the critical segregation

PLEASE CITE THIS ARTICLE AS DOI: 10.1063/5.0173047

Assessment of the Partial Saddle Point Approximation in Field-Theoretic Polymer Simulations

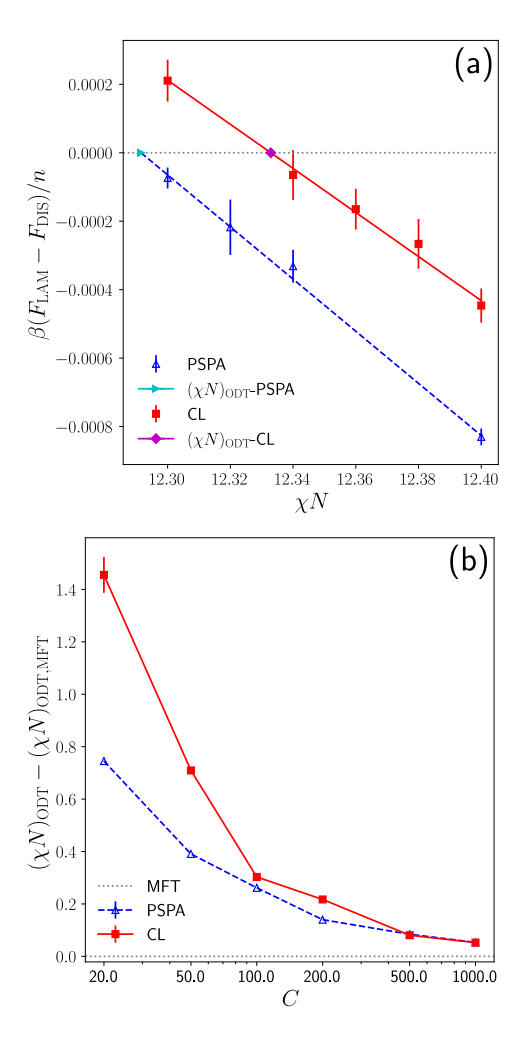


FIG. 4: Comparision of order-disorder transitions obtained using complex Langevin sampling (CL) and the partial saddle point approximation (PSPA) at $\zeta N = 100$. (a) The ODT is located by the zero crossing of the free energy difference between LAM and disordered phases at C = 100. (b) ODT shift relative to numerical SCFT as a function of chain concentration C.

strength.

In applying the direct free energy method, the cell size of the LAM phase is adjusted until the internal stress becomes isotropic. Besides serving as a precursor to free energy calculations, the "stress-free" cell size results in an immediate estimate of the equilibrium microdomain period D. To this end, we have computed the microdomain period of the LAM phase at $\chi N=20.0$ with $\alpha=0.2R_g$, ζN ranging from 50-500, and C spanning 5-100.

Figure 5 shows the fluctuation correction to the domain spacing, $\Delta D = D - D_{\text{MFT}}$, where D_{MFT} is the mean-field domain spacing determined from SCFT. As shown previously by Fredrickson

PLEASE CITE THIS ARTICLE AS DOI: 10.1063/5.0173047

Assessment of the Partial Saddle Point Approximation in Field-Theoretic Polymer Simulations

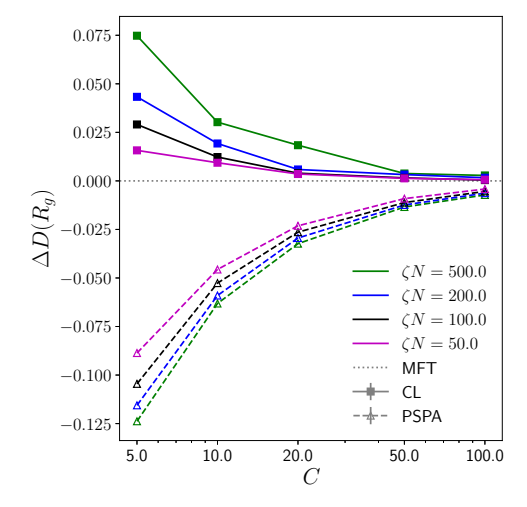


FIG. 5: Concentration dependence of the equilibrium microdomain period of the LAM phase relative to the mean-field/SCFT prediction, $\Delta D = D - D_{\rm MFT}$, computed both with CL and PSPA. The segregation strength is fixed at $\chi N = 20.0$ and the lines are guides to the eye.

and Delaney,¹⁴ CL sampling of field fluctuations results in a small positive displacement of the LAM microdomain period relative to the SCFT value. This fluctuation enhancement of D is seen to increase with decreasing C or compressibility $1/(\zeta N)$ and is consistent in sign with analytical theory.⁶¹ In contrast, the partial saddle point approximation predicts domain *contraction* rather than domain expansion. This qualitative failing of the PSPA is evidently a consequence of truncating the full field fluctuation spectrum of the repulsive mode w_+ .

IV. DISCUSSION

The results presented above for the regularized weakly-compressible model, Model II, demonstrated, both qualitatively and quantitatively, that the predictions emerging from the partial saddle point approximation (PSPA) are not thermodynamically consistent with those of the full theory. Nonetheless, Model II is not the model that is typically used in conjunction with the PSPA. The PSPA is traditionally applied to the unregularized incompressible model (Model I), whose UV divergences are addressed using a lattice cutoff in conjunction with a renormalization strategy known as Morse calibration. ^{19,26,50} With this in mind, we conducted a more limited study comparing PSPA and CL in the incompressible melt model, which is included in the supplementary material.

The results presented above for the regularized weakly-compressible model, Model II, demon-

PLEASE CITE THIS ARTICLE AS DOI: 10.1063/5.0173047

strated, both qualitatively and quantitatively, that the predictions emerging from the partial saddle point approximation (PSPA) are not thermodynamically consistent with those of the full theory. Nonetheless, Model II is not the model that is typically used in conjunction with the PSPA. The PSPA is traditionally applied to the unregularized incompressible model (Model I), whose UV divergences are addressed using a lattice cutoff in conjunction with a renormalization strategy known as Morse calibration. 19,26,50 With this in mind, we conducted a more limited study comparing PSPA and CL in the incompressible melt model, which is included in the supplementary material.

For the supplementary investigation, the Gaussian fluctuation formulas appropriate for Model I were derived from those for Model II by taking the dual limits $\zeta N \to \infty$ and $a \to 0$. This would nominally produce singular terms in the free energy, but it is straightforward to see that they can be cancelled by substracting the same formula in the reference state of $\chi N = 0$. This regularization procedure for the incompressible model effectively removes contributions from the w_{+} mode, curiously leading to the same result for the PSPA and the full theory in the symmetric case of $f = 0.5,^{26,62}$

$$\frac{\beta \Delta F}{n} = \frac{1}{4\pi^2 C} \int_0^\infty dk \, k^2 \ln\left[1 - \chi N\left(\hat{g}_{AA}(k^2) - \hat{g}_{AB}(k^2)\right)\right] \tag{42}$$

As in Fig. 2, $\beta \Delta F/n$ is defined as the fluctuation contribution of the intensive Helmholtz free energy that has had ideal gas, mean-field, and reference state contributions removed. This analytical result suggests that the PSPA may be accurate in predicting fluctuation corrections to the regularized Helmholtz free energy in the incompressible limit, as has been tacitly assumed without rigorous demonstration in the literature. ^{15–21,27} In Figure S2, we compare $\beta \Delta F/n$ obtained from the Gaussian fluctuation analysis of Eq. (42) with numerical results obtained from PSPA and CL simulations. The simulation data from the two methods are in semi-quantitative agreement across a range of C, and significantly deviate from the analytical Gaussian formula only below $C \approx 100$. Overall, we conclude that the primitive regularization scheme of subtracting a reference state is remarkably effective at minimizing the difference between PSPA and CL free energy predictions for the standard incompressible, unsmeared Model I. We speculate that lattice cutoff and Morse calibration would produce a similar effect.

The periodic domain contraction trend noticed by the PSPA for Model II appears to be contrary to both analytical theory^{61,63} and weakly-compressible CL simulations¹⁴. Previous works present disordered phase structure factors S(k) and show decreases in the location of the primary peak k^*

PLEASE CITE THIS ARTICLE AS DOI: 10.1063/5.0173047

Assessment of the Partial Saddle Point Approximation in Field-Theoretic Polymer Simulations

as C decreases. The peak location is expected to approximately set the periodic domain spacing in the weakly ordered lamellar phase according to $D = 2\pi/k^*$. The analytical results suggest and the simulation results confirm for Model II that decreasing C increases the domain spacing D to accommodate stronger field fluctuations. Figure S3 shows that domain contraction is observed in the incompressible Model I for both the PSPA and CL simulations. Such contraction has been previously seen in PSPA-based simulations, ^{24,57} but Figure S3 shows that PSPA applied to a model with no regularization (bare parameters) significantly overestimates the contraction relative to CL. These findings for Model I further support our assertion that the domain contraction seen in the PSPA results for Model II is a consequence of the suppression of the repulsive mode w_+ .

Within the confines of Model I, the ultraviolet divergences can be suppressed using a technique known as Morse calibration. 50,51 Morse calibration regularizes the UV divergent model by renormalizing both the interaction parameter χ and the statistical segment length b, thus adjusting both the relevant lengthscale R_g and the Ginzburg parameter C. With Morse calibration, PSPA simulations of Model I produce results that demonstrate remarkably good agreement with particle-based simulations that have undergone calibration as well. These results closely align the two sets of simulations' free energy values, order-disorder transition locations, and periodic domain spacing. 26,42 Our findings reinforce the fact that, without Morse calibration, the PSPA approximation breaks down for incompressible diblocks in domain spacing predictions. This requirement of regularization in applying the PSPA is likely even more pronounced for incompressible/contact models of complex architecture systems (such as bottlebrush polymers) that undergo fluctuation-induced backbone stiffening. 22,33,64,65 Unfortunately, Morse calibration theory has not been extended to date to such broader classes of single and multicomponent systems. 66,67

V. CONCLUSION

This work is the first comprehensive comparison of field-theoretic simulation methods that employ the partial saddle point approximation (PSPA) against complex Langevin (CL) methods that invoke no simplifying approximation. The PSPA removes the sign problem in sampling the field theory at the cost of admitting an uncontrolled approximation. We have primarily compared the PSPA with the full theory (CL) using a weakly-compressible model of symmetric AB diblock copolymers with finite-range interactions that is free of ultraviolet (UV) divergences. It was found both numerically and analytically that the PSPA in the weakly-inhomogenous regime predicts in-

PLEASE CITE THIS ARTICLE AS DOI: 10.1063/5.0173047

Assessment of the Partial Saddle Point Approximation in Field-Theoretic Polymer Simulations

correct trends in the fluctuation contribution to the free energy, predicting negative rather than positive corrections to the mean field reference. The PSPA also underestimates the critical segregation strength for the order-disorder transition and forms more strongly ordered phases. In the lamellar phase, the PSPA incorrectly predicts domain period contraction rather than expansion. These results were augmented by numerical and analytical assessments of the PSPA in a "standard" incompressible model with contact interactions that is UV-divergent. Our analysis indicates that the PSPA is most appropriate in the incompressible limit where deviations with field-theoretic simulations based on CL sampling are smallest.

SUPPLEMENTARY MATERIAL

The supplementary material includes details regarding the Gaussian fluctuations analysis used in this work. In addition, a more limited study comparing PSPA and CL in the incompressible melt model (Model I) is also included in the supplementary material.

ACKNOWLEDGMENTS

The authors thank Kevin Shen, Doug Grzetic, Kaitlin Albanese, and Daniel Vigil for stimulating discussions. This work was supported by the CMMT Program of the National Science Foundation under grant no. DMR-2104255. T.Q. acknowledges support from the National Science Foundation Graduate Research Fellowship Program under grant no. 1650114. Any opinions, findings, and conclusions or recommendations expressed in this material are those of the author(s) and do not necessarily reflect the views of the National Science Foundation. Use was made of computational facilities purchased with funds from the National Science Foundation (CNS-1725797) and administered by the Center for Scientific Computing (CSC). The CSC is supported by the California NanoSystems Institute and the Materials Research Science and Engineering Center (MRSEC; NSF DMR 2308708) at UC Santa Barbara.

AUTHOR DECLARATIONS

Conflict of Interest

The authors have no conflicts to disclose.

PLEASE CITE THIS ARTICLE AS DOI: 10.1063/5.0173047

Assessment of the Partial Saddle Point Approximation in Field-Theoretic Polymer Simulations

Author Contributions

Timothy Quah: Conceptualization (equal); Data curation (lead); Formal analysis (lead); Investigation (lead); Methodology (equal); Visualization (lead); Software (equal); Writing – original draft (lead). Kris T. Delaney: Conceptualization (equal); Methodology (equal); Software (equal); Supervision (equal); Writing – review & editing (equal); Resources(equal). Glenn H. Fredrickson: Conceptualization (equal); Funding acquisition (lead); Methodology (equal); Supervision (equal); Writing – review & editing (lead); Resources (equal).

DATA AVAILABILITY STATEMENT

The data that supports the findings of this study are available within the article and its supplementary material.

REFERENCES

- 1 M. W. Matsen, "Self-consistent field theory and its applications," Sons, Soft Matter (John Wiley & Ltd, 2005) Chap. 2, pp. 87-178, https://onlinelibrary.wiley.com/doi/pdf/10.1002/9783527617050.ch2.
- ²F. Schmid, Journal of Physics: Condensed Matter **10**, 8105 (1998), https://dx.doi.org/10.1088/0953-8984/10/37/002.
- ³M. W. Matsen, Journal of Physics: Condensed Matter **14**, R21 (2001), https://dx.doi.org/10.1088/0953-8984/14/2/201.
- ⁴G. Fredrickson, *The Equilibrium Theory of Inhomogeneous Polymers* (Oxford University Press, 2005) https://doi.org/10.1093/acprof:oso/9780198567295.001.0001.
- ⁵A. Arora, J. Qin, D. C. Morse, K. T. Delaney, G. H. Fredrickson, F. S. Bates, and K. D. Dorfman, Macromolecules **49**, 4675 (2016), https://doi.org/10.1021/acs.macromol.6b00107.
- ⁶G. H. Fredrickson, V. Ganesan, and F. Drolet, Macromolecules **35**, 16 (2002), https://doi.org/10.1021/ma011515t.
- ⁷G. H. Fredrickson and K. T. Delaney, *Field-Theoretic Simulations in Soft Matter and Quantum Fluids* (Oxford University Press, 2023) https://academic.oup.com/book/45705/book-pdf/50133196/9780192663238_web.pdf.

PLEASE CITE THIS ARTICLE AS DOI: 10.1063/5.0173047

Assessment of the Partial Saddle Point Approximation in Field-Theoretic Polymer Simulations

- ⁸M. W. Matsen, The Journal of Chemical Physics **152**, 110901 (2020), https://doi.org/10.1063/1.5145098.
- ⁹M. W. Matsen and T. M. Beardsley, Polymers **13** (2021), 10.3390/polym13152437, https://www.mdpi.com/2073-4360/13/15/2437.
- ¹⁰E. M. Lennon, G. O. Mohler, H. D. Ceniceros, C. J. García-Cervera, and G. H. Fredrickson, Multiscale Modeling & Simulation 6, 1347 (2008), https://doi.org/10.1137/070689401.
- ¹¹M. C. Villet and G. H. Fredrickson, The Journal of Chemical Physics **141**, 224115 (2014), https://doi.org/10.1063/1.4902886.
- ¹²D. Düchs, K. T. Delaney, and G. H. Fredrickson, The Journal of Chemical Physics **141**, 174103 (2014), https://doi.org/10.1063/1.4900574.
- ¹³K. T. Delaney and G. H. Fredrickson, The Journal of Physical Chemistry B **120**, 7615 (2016), pMID: 27414265, https://doi.org/10.1021/acs.jpcb.6b05704.
- ¹⁴G. H. Fredrickson and K. T. Delaney, Proceedings of the National Academy of Sciences **119**, e2201804119 (2022), https://www.pnas.org/doi/pdf/10.1073/pnas.2201804119.
- ¹⁵D. Yong and J. U. Kim, Macromolecules **55**, 6505 (2022), https://doi.org/10.1021/acs.macromol.2c00705.
- ¹⁶B. Vorselaars, The Journal of Chemical Physics **158**, 114117 (2023), https://pubs.aip.org/aip/jcp/article-pdf/doi/10.1063/5.0131183/16792533/114117_1_online.pdf.
- ¹⁷P. Stasiak and M. W. Matsen, Macromolecules **46**, 8037 (2013), https://doi.org/10.1021/ma401687j.
- ¹⁸T. M. Beardsley, R. K. W. Spencer, and M. W. Matsen, Macromolecules **52**, 8840 (2019), https://doi.org/10.1021/acs.macromol.9b01904.
- ¹⁹T. M. Beardsley and M. W. Matsen, The Journal of Chemical Physics **150**, 174902 (2019), https://pubs.aip.org/aip/jcp/article-pdf/doi/10.1063/1.5089217/13777228/174902_1_online.pdf.
- ²⁰R. K. W. Spencer, B. Vorselaars, and M. W. Matsen, Macromolecular Theory and Simulations **26**, 1700036 (2017), https://onlinelibrary.wiley.com/doi/pdf/10.1002/mats.201700036.
- ²¹A. Alexander-Katz and G. H. Fredrickson, Macromolecules **40**, 4075 (2007), https://doi.org/10.1021/ma070005h.
- ²²M. W. Bates, J. Lequieu, S. M. Barbon, R. M. Lewis, K. T. Delaney, A. Anastasaki, C. J. Hawker, G. H. Fredrickson, and C. M. Bates, Proceedings of the National Academy of Sciences 116, 13194 (2019), https://www.pnas.org/doi/pdf/10.1073/pnas.1900121116.

PLEASE CITE THIS ARTICLE AS DOI: 10.1063/5.0173047

Assessment of the Partial Saddle Point Approximation in Field-Theoretic Polymer Simulations

- ²³T. M. Beardsley and M. W. Matsen, The Journal of Chemical Physics **154**, 124902 (2021), https://doi.org/10.1063/5.0046167.
- ²⁴R. K. W. Spencer and M. W. Matsen, The Journal of Chemical Physics **149**, 184901 (2018), https://doi.org/10.1063/1.5051744.
- ²⁵G. K. Cheong and K. D. Dorfman, Macromolecules **54**, 9868 (2021), https://doi.org/10.1021/acs.macromol.1c01629.
- ²⁶M. W. Matsen, T. M. Beardsley, and J. D. Willis, The Journal of Chemical Physics **158**, 044904 (2023), https://doi.org/10.1063/5.0134890.
- ²⁷D. Düchs, V. Ganesan, G. H. Fredrickson, and F. Schmid, Macromolecules **36**, 9237 (2003), https://doi.org/10.1021/ma030201y.
- ²⁸R. K. W. Spencer and M. W. Matsen, Macromolecules **54**, 1329 (2021), https://doi.org/10.1021/acs.macromol.0c02668.
- ²⁹B. Vorselaars, R. K. W. Spencer, and M. W. Matsen, Phys. Rev. Lett. **125**, 117801 (2020), https://link.aps.org/doi/10.1103/PhysRevLett.125.117801.
- ³⁰Y.-X. Liu, K. T. Delaney, and G. H. Fredrickson, Macromolecules **50**, 6263 (2017), https://doi.org/10.1021/acs.macromol.7b01106.
- ³¹J. Lequieu, T. Koeper, K. T. Delaney, and G. H. Fredrickson, Macromolecules **53**, 513 (2020), https://doi.org/10.1021/acs.macromol.9b02254.
- ³²D. J. Grzetic, K. T. Delaney, and G. H. Fredrickson, ACS Macro Letters 8, 962 (2019), pMID:
 35619489, https://doi.org/10.1021/acsmacrolett.9b00316.
- ³³E. Panagiotou, K. T. Delaney, and G. H. Fredrickson, The Journal of Chemical Physics **151**, 094901 (2019), https://doi.org/10.1063/1.5114698.
- ³⁴J. Lee, Y. O. Popov, and G. H. Fredrickson, The Journal of Chemical Physics **128**, 224908 (2008), https://doi.org/10.1063/1.2936834.
- ³⁵Y. O. Popov, J. Lee, and G. H. Fredrickson, Journal of Polymer Science Part B: Polymer Physics **45**, 3223 (2007), https://onlinelibrary.wiley.com/doi/pdf/10.1002/polb.21334.
- ³⁶K. T. Delaney and G. H. Fredrickson, The Journal of Chemical Physics **146**, 224902 (2017), https://doi.org/10.1063/1.4985568.
- ³⁷J. McCarty, K. T. Delaney, S. P. O. Danielsen, G. H. Fredrickson, and J.-E. Shea, The Journal of Physical Chemistry Letters **10**, 1644 (2019), https://doi.org/10.1021/acs.jpclett.9b00099.
- ³⁸S. P. O. Danielsen, J. McCarty, J.-E. Shea, K. T. Delaney, and G. H. Fredrickson, Proceedings of the National Academy of Sciences **116**, 8224 (2019),

PLEASE CITE THIS ARTICLE AS DOI: 10.1063/5.0173047

- Assessment of the Partial Saddle Point Approximation in Field-Theoretic Polymer Simulations
 - https://www.pnas.org/doi/pdf/10.1073/pnas.1900435116.
- ³⁹G. H. Fredrickson, V. Ganesan, and F. Drolet, Macromolecules **35**, 16 (2002), https://doi.org/10.1021/ma011515t.
- ⁴⁰Z.-G. Wang, Macromolecules **28**, 570 (1995), https://doi.org/10.1021/ma00106a022.
- ⁴¹F. S. Bates, J. H. Rosedale, and G. H. Fredrickson, The Journal of Chemical Physics **92**, 6255 (1990), https://doi.org/10.1063/1.458350.
- ⁴²P. Medapuram, J. Glaser, and D. C. Morse, Macromolecules **48**, 819 (2015), https://doi.org/10.1021/ma5017264.
- ⁴³F. S. Bates, M. F. Schulz, A. K. Khandpur, S. Förster, J. H. Rosedale, K. Almdal, and K. Mortensen, Faraday Discuss. **98**, 7 (1994), http://dx.doi.org/10.1039/FD9949800007.
- ⁴⁴F. S. Bates, J. H. Rosedale, G. H. Fredrickson, and C. J. Glinka, Phys. Rev. Lett. **61**, 2229 (1988), https://link.aps.org/doi/10.1103/PhysRevLett.61.2229.
- ⁴⁵T. M. Gillard, P. Medapuram, D. C. Morse, and F. S. Bates, Macromolecules **48**, 2801 (2015), https://doi.org/10.1021/acs.macromol.5b00277.
- ⁴⁶S. Lee, Nuclear Physics B **413**, 827 (1994), https://doi.org/10.1016/0550-3213(94)90015-9.
- ⁴⁷W. J. Schoenmaker, Phys. Rev. D **36**, 1859 (1987), https://link.aps.org/doi/10.1103/PhysRevD.36.1859.
- ⁴⁸D. L. Vigil, K. T. Delaney, and G. H. Fredrickson, Macromolecules **54**, 9804 (2021), https://doi.org/10.1021/acs.macromol.1c01804.
- ⁴⁹E. M. Lennon, K. Katsov, and G. H. Fredrickson, Phys. Rev. Lett. **101**, 138302 (2008), https://link.aps.org/doi/10.1103/PhysRevLett.101.138302.
- ⁵⁰J. Glaser, P. Medapuram, T. M. Beardsley, M. W. Matsen, and D. C. Morse, Phys. Rev. Lett. **113**, 068302 (2014), https://link.aps.org/doi/10.1103/PhysRevLett.113.068302.
- ⁵¹J. Glaser, J. Qin, P. Medapuram, and D. C. Morse, Macromolecules **47**, 851 (2014), https://doi.org/10.1021/ma401694u.
- ⁵²Z.-G. Wang, Phys. Rev. E **81**, 021501 (2010), https://link.aps.org/doi/10.1103/PhysRevE.81.021501.
- ⁵³D. A. Hajduk, S. M. Gruner, S. Erramilli, R. A. Register, and L. J. Fetters, Macromolecules **29**, 1473 (1996), https://doi.org/10.1021/ma950643c.
- ⁵⁴E. Helfand, The Journal of Chemical Physics **62**, 999 (1975), https://doi.org/10.1063/1.430517.
- ⁵⁵S. Cox and P. Matthews, J. Comput. Phys. **176**, 430 (2002), http://www.sciencedirect.com/science/article/pii/S0021999102969950.

PLEASE CITE THIS ARTICLE AS DOI: 10.1063/5.0173047

Assessment of the Partial Saddle Point Approximation in Field-Theoretic Polymer Simulations

- ⁵⁶M. C. Villet and G. H. Fredrickson, The Journal of Chemical Physics **132**, 034109 (2010), https://pubs.aip.org/aip/jcp/article-pdf/doi/10.1063/1.3289723/15669136/034109_1_online.pdf.
- ⁵⁷B. Vorselaars, P. Stasiak, and M. W. Matsen, Macromolecules **48**, 9071 (2015), https://doi.org/10.1021/acs.macromol.5b02286.
- ⁵⁸K. Ø. Rasmussen and G. Kalosakas, J. Polym. Sci., Part B: Polym. Phys. **40**, 1777 (2002), https://onlinelibrary.wiley.com/doi/pdf/10.1002/polb.10238.
- ⁵⁹G. Tzeremes, K. Ø. Rasmussen, T. Lookman, and A. Saxena, Phys. Rev. E **65**, 041806 (2002), https://link.aps.org/doi/10.1103/PhysRevE.65.041806.
- ⁶⁰D. J. Grzetic, K. T. Delaney, and G. H. Fredrickson, The Journal of Chemical Physics **148** (2018), 10.1063/1.5025720, 204903, https://pubs.aip.org/aip/jcp/article-pdf/doi 10.1063/1.5025720/15545632/204903_1_online.pdf.
- ⁶¹J. Barrat and G. H. Fredrickson, The Journal of Chemical Physics **95**, 1281 (1991), https://doi.org/10.1063/1.461109.
- ⁶²M. Olvera de la Cruz, S. F. Edwards, and I. C. Sanchez, The Journal of Chemical Physics **89**, 1704 (1988), https://doi.org/10.1063/1.455116.
- ⁶³A. M. Mayes and M. O. de la Cruz, The Journal of Chemical Physics **95**, 4670 (1991), https://doi.org/10.1063/1.461736.
- ⁶⁴S. J. Dalsin, T. G. Rions-Maehren, M. D. Beam, F. S. Bates, M. A. Hillmyer, and M. W. Matsen, ACS Nano **9**, 12233 (2015), pMID: 26544636, https://doi.org/10.1021/acsnano.5b05473.
- ⁶⁵J. Park, V. Thapar, Y. Choe, L. A. Padilla Salas, A. Ramírez-Hernández, J. J. de Pablo, and S.-M. Hur, ACS Macro Letters 11, 1167 (2022), pMID: 36083506, https://doi.org/10.1021/acsmacrolett.2c00310.
- 66 V. Sethuraman, B. H. and V. Ganesan, The Nguyen, Journal of 141, Chemical **Physics** 244904 (2014),https://pubs.aip.org/aip/jcp/articlepdf/doi/10.1063/1.4904390/15493106/244904_1_online.pdf.
- ⁶⁷J. Qin and D. C. Morse, Phys. Rev. Lett. **108**, 238301 (2012), https://link.aps.org/doi/10.1103/PhysRevLett.108.238301.